

Cite this: *Chem. Commun.*, 2011, **47**, 11312–11314

www.rsc.org/chemcomm

## COMMUNICATION

Scanning tunneling microscopy/spectroscopy on self-assembly of a glycine/Cu(111) nanocavity array<sup>†‡</sup>

Ken Kanazawa, Atsushi Taninaka, Hui Huang, Munenori Nishimura, Shoji Yoshida, Osamu Takeuchi and Hidemi Shigekawa\*

Received 31st March 2011, Accepted 5th September 2011

DOI: 10.1039/c1cc11829c

The step-by-step analysis of a hierarchical self-assembly revealed the incorporation of nanocavity blocks in a metastable orientation to stabilize the organized array. The confinement of 2D electrons by a quantum corral was verified. Furthermore, manipulation of an isolated C<sub>60</sub> molecule was realized using nanocavities of ~1.3 nm diameter as a template.

The engineering of nanostructures through the self-assembly of organic molecules is a key factor in the development of future functional devices.<sup>1</sup> Because of the advantages of real-space analysis with atomic resolution, adsorbed molecules on solid surfaces have been extensively studied by scanning tunneling microscopy/spectroscopy (STM/STS), which provides valuable information not only on structures and formation processes<sup>2,3</sup> but also on their functional properties originating from their molecular and surface electronic structures.<sup>4</sup> Furthermore, STM enables the manipulation of molecular structures and functions,<sup>5</sup> providing information on their dynamical processes of interest from fundamental and practical viewpoints.

In the interactive dynamics of molecules on a solid surface, footprint chirality, *i.e.*, the chirality determined after the adsorption of molecules, plays an important role in providing a driving force to realize functions by multistep processes *via* the formation of multimer units.<sup>3,6</sup> Among the naturally occurring  $\alpha$ -amino acids, glycine is the only molecule that does not have chirality, although enantiomeric isomers appear on a metal at room temperature (RT) through the dissociation of hydrogen from the carboxyl group, depending on the freedom of the directional relationship between the two groups in the adsorbed form (molecules in *R*- and *S*-trimers in Fig. 1(b)).<sup>7</sup> Since only two footprints with the same formation energy are created, glycine provides a simple example to study the interactive dynamics in self-assembly.

Here, we present the results obtained by STM/STS for a glycine/Cu(111) self-assembly.

Institute of Applied Physics, University of Tsukuba, 305-8573 Tsukuba, Japan. E-mail: hidemi@ims.tsukuba.ac.jp; Web: <http://dora.bk.tsukuba.ac.jp>; Fax: +81 29 853 6469; Tel: +81 29 853 6469

<sup>†</sup> Electronic supplementary information (ESI) available. See DOI: 10.1039/c1cc11829c

<sup>‡</sup> This article is part of the *ChemComm* 'Molecule-based surface chemistry' web themed issue.

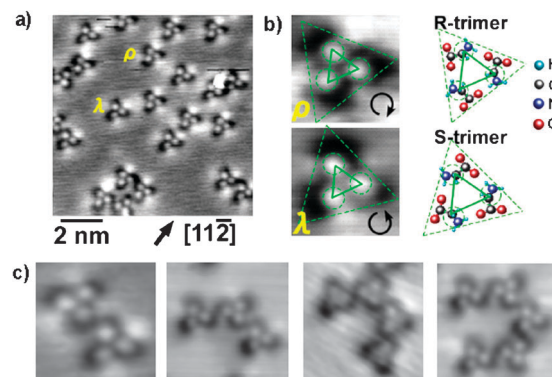


**Fig. 1** (a) STM image of isolated glycine trimers (sample voltage:  $V_s = +0.5$  V, tunneling current:  $I_t = 1.0$  nA).  $\rho$  and  $\lambda$  indicate two types of enantiomeric trimer. (b) Magnified STM images of the trimers A and B in (a) and their schematic illustrations (●: H, ●: O, ●: N, ●: C). Solid and dotted green triangles are drawn for comparison. (c) STM images of step-by-step homochiral-ring-formation of glycine trimers.

After molecular deposition on a clean Cu(111) surface, the sample was annealed at 350 K for 1 h.<sup>7</sup> Then, STM/STS measurements were performed in ultrahigh vacuum ( $< 1 \times 10^{-8}$  Pa) at 5 K using a tungsten tip.

Fig. 1(a) shows an STM image of a surface covered with a thin layer of glycine molecules ( $< 0.2$  molecular layer (ML)). Some triangular structures can be observed. Each side of the triangle is about 1 nm, which is much larger than the size of a single glycine molecule. The triangles consist of three bright spots with the same brightness surrounded by regions of depression that are darker than the original substrate. By considering their directional relationships with the threefold rotational symmetry of the Cu(111) surface, the triangular structures are divided into two types with a mirror plane along the  $[11\bar{2}]$  direction labeled as  $\rho$  and  $\lambda$  in Fig. 2(a). Our STM images indicate the existence of enantiomeric isomers forming the supramolecular trimers, *i.e.*, each triangular structure consists of three homochiral glycinate molecules, resulting in the two types described above. By considering the threefold rotational symmetry of the substrate and the hydrogen bonding between the amino and carboxyl groups, which have been observed in the self-assembly of glycine/Cu(100),<sup>6,8</sup> schematic structures of the two types of homochiral glycinate trimers (*R*- and *S*-trimers) were developed. The methylene groups and the Cu areas near the

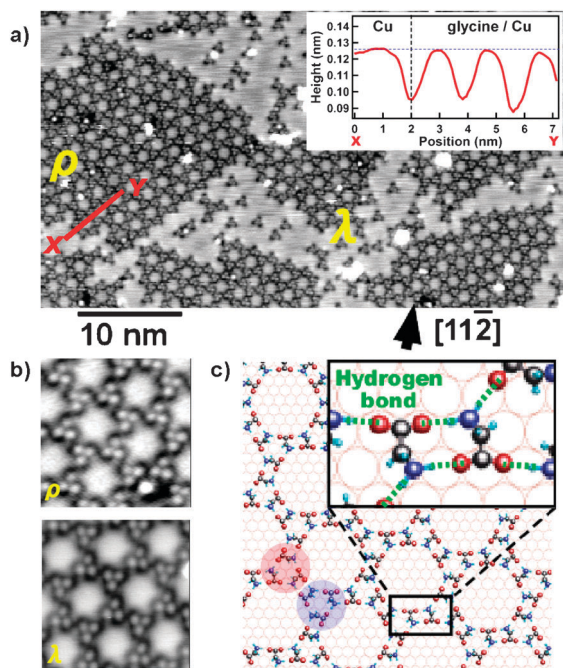


**Fig. 2** (a) STM image of self-assembled network of glycine trimers ( $V_s = -0.5$  V,  $I_t = 0.5$  nA) and the cross-section along  $X$ - $Y$ . (b) High-resolution STM images of  $\rho$  and  $\lambda$  in (a), and (c) schematic of the molecular arrangement of structure  $\rho$  (●: H, ●: O, ●: N, ●: C). The green dotted lines in the box show the hydrogen bonds between molecules.

carboxyl groups are attributed to the brightest points and the regions of depression, respectively, which is discussed in ESI†

Fig. 1(c) shows the homochiral-ring formation of the glycine trimers observed, suggesting the formation of a higher-order structure based on the trimer units. In fact, for a larger coverage of glycine molecules ( $\sim 0.5$  ML), a network of trimers appeared that formed an array of nanoscale cavities of  $\sim 1.3$  nm diameter (Fig. 2(a)). The structure has  $2\sqrt{13} \times 2\sqrt{13}$ -R13.9° periodicity. As shown by the domains  $\rho$  and  $\lambda$  in Fig. 2(a) and their magnifications (Fig. 2(b)), there are two structures with a  $[11\bar{2}]$  mirror plane, which consist of circularly ordered trimers with homochiralities indicated by  $\rho$  and  $\lambda$  in Fig. 1(b). The enantioselectivity observed in the formation of trimer units also plays an important role in the growth of the large-scale network.

For the  $2\sqrt{13} \times 2\sqrt{13}$  structure previously reported, a double-ring model was proposed.<sup>9</sup> However, as shown by the cross-section in Fig. 2(a), both the inside and outside regions of the nanocavity have similar heights, suggesting that the bottom surface in the nanocavity is also a bare Cu surface. Since STM images depend on the bias voltage, we carried out STS to clarify the molecular structure observed in Fig. 2. Fig. 3(a) shows  $dI/dV$ - $V$  curves obtained in the substrate Cu(111) area (S) and at the center of a nanocavity (G). The two curves are different; however, the value of  $V_s \approx -0.4$  V, from which the difference between the two curves originates, is close to the minimum energy of the free-electron-like Cu(111) surface state,<sup>10</sup> suggesting that both regions are bare Cu surfaces and that the difference in Fig. 3(a) is due to the confinement of free electrons in the nanocavity.

Fig. 3(b) and (c) show  $dI/dV$  images obtained at various sample bias voltages. As expected, the  $dI/dV$  maps clearly reflect the electronic structures of the Cu(111) surface state confined by

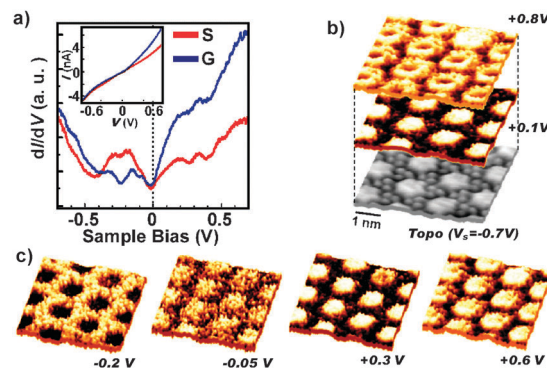


**Fig. 3** (a)  $dI/dV$ - $V$  and  $I$ - $V$  (inset) obtained at the substrate (S) and the center of a nanocavity (G) (set point:  $V_s = -0.5$  V,  $I_t = 0.5$  nA). (b) and (c)  $dI/dV$  maps for the voltage range of  $-0.2$  to  $+0.8$  V (set point:  $V_s = -0.25$  V,  $I_t = 0.5$  nA, grid:  $128 \times 128$ ).

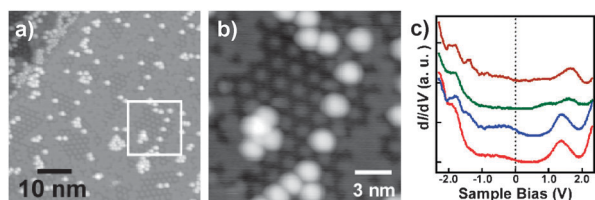
a single ring. At  $V_s = \sim +0.8$  V, the center of the nanocavity is dark with a bright circular edge with a diameter smaller than that of the nanocavity, providing an apparent image of the double-ring model; however, at  $V_s = \sim +0.1$  V, a bright state appears in the nanocavity. These are the second and ground states of the confined electrons, respectively (see ESI†).

Fig. 2(c) shows the structural model for the network. Neighboring trimers represented by blue and red circles exhibit  $180^\circ$  rotational symmetry. Since there are few isolated  $180^\circ$ -rotated  $\rho$  and  $\lambda$  trimers, as shown in Fig. 1(a), the isolated trimers are initially stabilized in accordance with the  $C_{3v}$  symmetry of the Cu(111) substrate surface. In the  $180^\circ$  rotational arrangement, each glycinate has four hydrogen bonds between the amino and carboxyl groups, enabling intra- and intertrimer coupling (dotted green lines in Fig. 2(c)) and producing strong interactions.

In the self-assembly of (*RS*)-3-pyrroline-2-carboxylic acid on Cu(110), the molecular chirality and adsorption footprints appear to play a similar role in organization despite their different conformation energies.<sup>3</sup> The results obtained for glycine/Cu(111) strongly indicate the importance of the footprint concept also in the hierarchical self-assembly. Understanding the interactive dynamics at both microscopic and nonlocal scales is important, and the step-by-step analysis, for example shown in Fig. 1(c), is effective for obtaining such an understanding.

Finally, we demonstrate the ability of the network structure as a template for fullerene molecules. Fullerenes and their derivatives on metal electrodes are prospective building blocks for functional nanostructures. However, at a low coverage, they are usually so mobile on the terraces of a metal surface that they easily diffuse towards step edges and form condensed structures.<sup>11,12</sup> Therefore, it is difficult to obtain the isolated molecular condition that is essential for achieving molecular devices.<sup>13</sup> To overcome this inherent problem, the use of templates has been studied.<sup>14</sup> The diameter of the nanocavities in the network is about 1.3 nm, enabling the use of the nanocavity structure to realize a structure with isolated  $C_{60}$  molecules on a Cu(111) surface.

Fig. 4(a) is an STM image of  $C_{60}$  molecules deposited on a glycine network structure at RT. Unlike the case without a glycine template, most of the  $C_{60}$  molecules were adsorbed on the terraces. As clearly shown in the magnified image in Fig. 4(b), each molecule is adsorbed near the center of the nanocavity,



**Fig. 4** (a) STM image of  $C_{60}$  molecules on a glycine/Cu(111) structure ( $V_s = -0.5$  V,  $I_t = 0.5$  nA). (b) Magnified image of the square in (a). (c)  $dI/dV$ - $V$  curves obtained on isolated  $C_{60}$  (set point: +2.0 V, 1.0 nA).

suggesting that  $C_{60}$  molecules are in direct contact with the Cu substrate surface. In fact, STS curves measured on the  $C_{60}$  molecules (Fig. 4(c)) exhibit a similar characteristic to that observed for  $C_{60}$  molecules adsorbed at a Cu(111) step edge.<sup>12,15</sup>

Fig. 5(a) shows the existence of two different states for the  $C_{60}$  molecules adsorbed on the template. They are distinguished as brighter protrusions ( $B_1$  and  $B_2$ ) and darker protrusions ( $D_1$  and  $D_2$ ) in Fig. 5(a), respectively. The difference in brightness between the two states is clearer in the cross-section shown in Fig. 5(c). The ratio of the number of molecules with the bright and dark states was 2:3, indicating that the darker state is the major and more stable state. As shown in the  $dI/dV$  image in

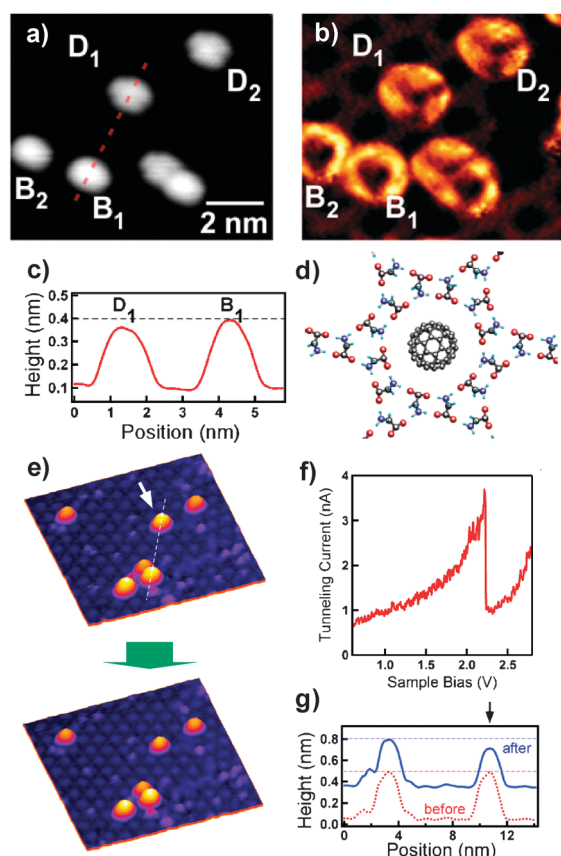


**Fig. 5** (a) and (b) STM ( $V_s = +1.5$  V,  $I_t = 0.5$  nA) and  $dI/dV$  ( $V_s = -1.5$  V,  $I_t = 0.5$  nA) images of the two states of adsorbed  $C_{60}$  molecules, indicated by  $B_1$  and  $B_2$  (bright) and by  $D_1$  and  $D_2$  (dark), respectively. (c) Cross-section along the red dashed line in (a). (d) Schematic illustration of the darker  $C_{60}$  molecule in the glycine nanocavity. (e) STM images obtained before and after excitation. (f)  $I$ - $V$  curve obtained for the molecule indicated by an arrow in (e). (g) Cross-sections obtained along the dotted line in (e) before (blue) and after (red) excitation ( $I$ - $V$  measurement).

Fig. 5(b), the molecule with the darker state has threefold rotational symmetry on the Cu(111) substrate. Therefore, each darker  $C_{60}$  molecule is adsorbed with its six-membered ring facing the substrate as schematically shown in Fig. 5(d), which is considered to be more stable than the configuration of the other state. The existence of two states due to a difference in the molecular orientation has also been reported for a molecular layer of condensed  $C_{60}$  on a Cu(111) surface.<sup>12</sup>

We manipulated isolated  $C_{60}$  using STM (Fig. 5(e)). We scanned an applied bias voltage with the STM tip placed above  $C_{60}$  in the brighter state, indicated by an arrow in Fig. 5(e). As shown in the  $I$ - $V$  curve in Fig. 5(f), the tunneling current suddenly dropped at  $V_s \approx +2.3$  V, indicating a change in the molecular state. According to the cross-section along the dotted line in Fig. 5(e) obtained before and after the excitation, the molecule indicated by an arrow underwent a transformation to the darker state, which is considered to be caused by the rotation of the molecule in the cavity (Fig. 5(g)). In this study, we only succeeded in inducing the transformation in one direction because of the high stability of the darker state. If a molecule such as an endohedral fullerene with an ellipsoid shape is used, the molecule will be located at a noncentral position in the nanocavity and may be reversibly controlled between different states, making the structure more applicable for molecular devices.

In conclusion, the formation of a quantum dot array and the successful manipulation of individual  $C_{60}$  show the potential of this system. The active use of the quantized states in the nanocavity with the combination of guest molecule may provide additional functions to realize electronic/optical devices.

## Notes and references

- C. Joachim, J. Gimzewski and A. Aviram, *Nature*, 2000, **408**, 541; J. Barth, *Annu. Rev. Phys. Chem.*, 2007, **58**, 175.
- J. Elemans, S. Lei and S. Feyter, *Angew. Chem., Int. Ed.*, 2009, **48**, 7298; O. Ivasenko, J. Macleod, K. Chernichenko, E. Balenkova, R. Shapanchenko, V. Neujdenko, F. Rosei and D. Perepichka, *Chem. Commun.*, 2009, 1192.
- L. Pérez-García and D. Amabilino, *Chem. Soc. Rev.*, 2007, **36**, 941; M. Forster, M. Dyer, S. Barrett, M. Persson and R. Raval, *J. Phys. Chem. C*, 2011, **115**, 1180.
- R. Temirov, S. Soubatch, A. Luican and F. S. Tautz, *Nature*, 2006, **444**, 350; T. Komeda, H. Isshiki, J. Liu, Y. Zhang, N. Lorente, K. Katoh, B. Breedlove and M. Yamashita, *Nat. Commun.*, 2011, **2**, 217.
- W. Ho, *J. Chem. Phys.*, 2002, **117**, 11033; Y. Sainoo, Y. Kim, T. Okawa, T. Komeda, H. Shigekawa and M. Kawai, *Phys. Rev. Lett.*, 2005, **95**, 246102.
- K. Kanazawa, A. Taninaka, O. Takeuchi and H. Shigekawa, *Phys. Rev. Lett.*, 2007, **99**, 216102.
- V. Efsthathiou and D. Woodruff, *Surf. Sci.*, 2003, **531**, 304.
- K. Kanazawa, Y. Sainoo, Y. Konishi, S. Yoshida, A. Taninaka, A. Okada, M. Berthe, N. Kobayashi, O. Takeuchi and H. Shigekawa, *J. Am. Chem. Soc.*, 2007, **129**, 740.
- X. Zhao, H. Yan, R. Zhao and W. Yang, *Langmuir*, 2003, **19**, 809.
- S. Kevan, *Phys. Rev. Lett.*, 1983, **50**, 526.
- T. Sakurai, X.-D. Wang, Q. Xue, Y. Hasegawa, T. Hashizume and H. Shinohara, *Prog. Surf. Sci.*, 1996, **51**, 263.
- C. Silien, N. Pradhan, W. Ho and P. Thiry, *Phys. Rev. B: Condens. Matter Mater. Phys.*, 2004, **69**, 115434.
- R. Nouchi, K. Masunari, T. Ohta, Y. Kubozono and Y. Iwasa, *Phys. Rev. Lett.*, 2006, **97**, 196101.
- L. Piot, F. Silly, L. Tortech, Y. Nicolas, P. Blanchard, J. Roncali and D. Fichou, *J. Am. Chem. Soc.*, 2009, **131**, 12864; H. Glowatzki, B. Brker, R.-P. Blum, O. Hofmann, A. Vollmer, R. Rieger, K. Müllen, E. Zojer, J. Rabe and N. Koch, *Nano Lett.*, 2008, **8**, 3825.
- J. Larsson, S. Elliot, J. Greer, J. Repp, G. Meyer and R. Allenspach, *Phys. Rev. B: Condens. Matter Mater. Phys.*, 2008, **77**, 115434.